Biochemical Pharmacology, Vol. 56, pp. 293–299, 1998.

ELSEVIER

ISSN 0006-2952/98/$19.00 + 0.00
PII S0006-2952(98)00035-5

Inhibition of Acetylcholinesterase and Butyrylcholinesterase by Chlorpyrifos-oxon

Gabriel Amitai,†‡ Deborah Moorad,* Rachel Adani† and B. P. Doctor**

*Division of Biochemistry, Walter Reed Army Institute of Research, Washington, DC 20307-5100, U.S.A.; and †Israel Institute for Biological Research, 74100 Ness-Ziona, Israel

ABSTRACT. Phosphorothionate insecticides such as parathion (*O*,*O*-diethyl *O*-*p*-nitrophenyl phosphorothioate) and chlorpyrifos (CPS; *O*,*O*-diethyl *O*-3,5,6-trichloro-2-pyridyl phosphorothioate; Dursban) are metabolically converted by oxidative desulfuration into paraoxon and chlorpyrifos-oxon (CPO). The insecticidal action of chlorpyrifos stems from inhibition of acetylcholinesterase (AChE) by CPO, resulting in severe cholinergic toxicity. Sensory peripheral neuropathy was observed in people exposed environmentally to chlorpyrifos sprayed in confined areas. We have examined the kinetics of inhibition of AChE and butyrylcholinesterase (BChE) by paraoxon and CPO. The bimolecular rate constants (k_i) for inhibition by paraoxon of recombinant human (rH) AChE, recombinant mouse (rM) AChE, and fetal bovine serum (FBS) AChE were 7.0, 4.0, and 3.2×10^5 M^{-1} min^{-1}. The k_i values for the inhibition by CPO of rH AChE, fetal bovine serum AChE, human RBC AChE, *Torpedo* AChE, and recombinant mouse (rM) AChE were 9.3, 2.2, 3.8, 8.0, and 5.1×10^6 M^{-1} min^{-1}, respectively. Inhibition of human serum BChE, rH BChE, and rM BChE by CPO yielded k_i values of 1.65, 1.67, and 0.78×10^9 M^{-1} min^{-1}, respectively. The k_i values obtained for BChE from various species were 160- to 750-fold larger than those of AChE from parallel sources. Inhibition of the single-site mutant $A_{328}Y$ of rH BChE by CPO displayed a 21-fold lower rate than that of wild-type rH BChE (k_i, 7.9×10^7 vs 1.67×10^9 M^{-1} min^{-1}). The double mutant of acyl pocket residues of rH AChE, $F_{295}L/F_{297}V$, was inhibited by CPO with a 150-fold larger k_i than wild type (1.5×10^9 vs 1.0×10^7 M^{-1} min^{-1}). The increased rate obtained with the double mutant displaying characteristics of the BChE active center provides a rationale for higher efficacy of CPO scavenging by BChE, compared with AChE. BIOCHEM PHARMACOL **56**;3:293–299, 1998. © 1998 Elsevier Science Inc.

KEY WORDS. acetylcholinesterase inhibition; butyrylcholinesterase inhibition; chlorpyrifos-oxon; insecticide; paraoxon

OP§ insecticides exert their toxicity by irreversible inhibition of AChE (EC 3.1.1.7) in the peripheral and central cholinergic nervous system. Inhibition of either AChE in RBC or BChE (EC 3.1.1.8) in plasma serves as a diagnostic tool for the risk assessment of exposure to toxic OPs and carbamates. Phosphorothionate insecticides such as parathion (*O*,*O*-diethyl *O*-*p*-nitrophenyl phosphorothioate) and CPS (*O*,*O*-diethyl *O*-3,5,6-trichloro 2-pyridyl phosphorothioate, Dursban) are metabolically converted by oxidative desulfuration into their corresponding oxo-analogues: paraoxon and CPO, respectively (Scheme 1) [1]. The insecticidal action of CPS stems from inhibition of AChE by CPO, resulting in severe cholinergic toxicity [2]. CPO is detoxified subsequently by A-esterase hydrolysis [3, 4]. Repeated dosing of CPS in adult hens at levels sufficient to cause significant loss in body weight as well as considerable inhibition of brain AChE and serum BChE results in a low level of inhibition (18%) of the brain neuropathy target NTE [5]. AChE and NTE from hen whole brain homogenate are inhibited by CPO with bimolecular rate constants of 1.5×10^7 and 1.4×10^5 M^{-1} min^{-1}, respectively [6]. Subchronic and chronic treatment with CPS in rats, fish, and chickens has shown no indications of OP-induced delayed neurotoxicity [5, 7, 8]. However, sensory peripheral neuropathy was observed in people who had been exposed environmentally to CPS sprayed in confined areas [9, 10]. The present study describes the kinetic pattern of inhibition by CPO of AChE and BChE from various species and certain mutants of rH AChE and rH BChE. In this study, we found that the inhibition rate of BChE from various species by CPO was markedly more rapid than that of AChE.

‡ Corresponding author: Dr. Gabriel Amitai, P.O. Box 19, Israel Institute for Biological Research, 74100 Ness-Ziona, Israel. Tel. 972-8-938-1565; FAX 972-8-938-1559; E-mail: amitai@iibr.gov.il.

§ *Abbreviations:* AChE, acetylcholinesterase; ATC, acetylthiocholine iodide; BChE, butyrylcholinesterase; BTC, butyrylthiocholine iodide; CPO, chlorpyrifos-oxon; CPS, chlorpyrifos, *O*,*O*-diethyl*O*-3,5,6-trichloro 2-pyridyl phosphorothioate, Dursban; DTNB, 5,5′-dithiobis(2-nitrobenzoic acid); FBS AChE, fetal bovine serum acetylcholinesterase; HS BChE, human serum butyrylcholinesterase; NTE, neurotoxic esterase; RBC, red blood cell; rH AChE, recombinant human acetylcholinesterase; rH BChE, recombinant human wild-type butyrylcholinesterase; rM AChE, recombinant mouse acetylcholinesterase; rM BChE, recombinant mouse butyrylcholinesterase; and OP, organophosphate.

Received 16 April 1997; accepted 16 December 1997.

CPO **PARAOXON**

SCHEME 1. Chemical structures of CPO and paraoxon.

MATERIALS AND METHODS

Chemicals

CPO was obtained as an analytical standard (AGR 203674) from the Dow/Elanco Chemical Co. Paraoxon, ATC, BTC, and DTNB were purchased from the Sigma Chemical Co.

Enzymes

Human BChE purified from plasma, using procainamide–Sepharose 4B affinity chromatography, was a gift from Dr. Y. Ashani. rH BChE and its single-site mutant, $A_{328}Y$, were a gift from Dr. O. Lockridge. rM AChE and rM BChE were gifts from Dr. P. Taylor. *Torpedo* AChE in its dimer form was a gift from Dr. I. Silman. Purified rH AChE, the single-site mutants $F_{295}A$, and $F_{297}A$, and the double mutant $F_{295}L/F_{297}V$ were prepared according to Ordentlich *et al.* [11] and were a gift of Dr. A. Shafferman. FBS AChE was purified as described previously [12]. Human RBC AChE was enriched using the same procedure.

AChE and BChE Activity Assay

AChE and BChE activities were measured according to the procedure of Ellman [13] with a 0.5-mM concentration of either ATC or BTC, 50 mM phosphate buffer, pH 8.0, using a Beckman spectrophotometer (25°). Because some of the recombinant enzyme samples had low activity, their activity was measured in 100-μL total reaction volume, using a Thermomax microplate reader at 25° (Molecular Devices).

Determination of K_m

As depicted in Scheme 2, the substrate interacts with the enzyme at two different sites. The first is at the catalytic site to form a productive complex, ES. A second reversible non-productive complex, SE, may be formed by binding at

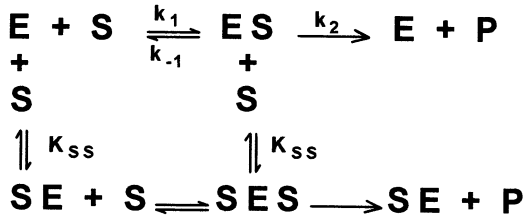

SCHEME 2. Equilibrium between either AChE and BChE (E) and their binary (ES) and ternary (SES) enzyme–substrate complexes.

the peripheral site distal from the catalytic triad. A ternary productive complex, ESE, could also be formed, where two substrate molecules bind simultaneously to one enzyme molecule.

K_m was determined by measuring the enzyme activity at various substrate concentrations. A nonlinear fit to the plot of v against S was performed using Eqn 1 [14]:

$$v = V_{max}(1 + b[S]/K_{ss})/(1 + [S]/K_{ss}) \cdot (1 + K_m/[S]) \quad (1)$$

where v and V_{max} are the enzyme activity and maximal activity, respectively; K_m is the Michaelis constant for the substrate–enzyme complex, ES; K_{ss} is the dissociation constant of substrate from SE or SES (binding at the peripheral site); b is the activation factor for BChE ($b > 1$) (or inhibition factor in the case of AChE, $b < 1$) for the ternary complex, ESE [15].

Inhibition Kinetics Using the Sampling Method

The enzyme (1.3 to 5 U/mL of either AChE or BChE) was incubated in the presence of various concentrations of inhibitors. At specified time intervals, 20-μL samples were added to 1 mL phosphate buffer containing 0.3 mM DTNB and 0.5 mM ATC (or 0.5 mM BTC) for the measurement of residual activity. The inhibition rate was followed by directly measuring the increase in absorbance at 412 nm. The pseudo-first-order rate constant, k_{obs}, was determined from the slope of the semi-logarithmic plot of fractional residual activity against time for a particular inhibitor concentration. The bimolecular rate constant of inhibition, k_i, was calculated from the double-reciprocal plot of $1/k_{obs}$ against 1/I (I = inhibitor concentration).

Inhibition Kinetics in the Presence of Substrate (Direct Method)

Some kinetic measurements were performed in the presence of substrate. This method was employed primarily for the inhibition of BChE by CPO. The rapid reaction of CPO with BChE necessitated the use of the direct method in which an aliquot of free enzyme was added to a solution containing 0.5 mM BTC (or ATC), 0.3 mM DTNB, and CPO at specified concentrations (see Table 3). The inhibition rate was followed by directly measuring the increase in absorbance at 412 nm. The pseudo-first-order kinetic rate constant, k_{obs}, was calculated from the semi-logarithmic plot of residual enzyme activity against time. This plot was obtained from the derivative function of the continuous reading of absorbance during a 2- to 5-min interval. Determination of the bimolecular rate constants for inhibition by CPO of HS BChE, rM BChE, rH BChE and its $A_{328}Y$ single mutant, and wild-type rH AChE and its mutants, $F_{295}A$, $F_{297}A$, and $F_{295}L/F_{297}V$, was performed using the double-reciprocal method of Hart and O'Brien [16], as detailed previously [17], using Eqn 2:

$$1/k_{obs} = K_d/k_2(1/[I](1 - \alpha)) + 1/k_2 \quad (2)$$

where k_2 is the first-order phosphorylation rate constant, K_d is the dissociation constant for the reversible complex between CPO and AChE, $\alpha = [S]/(K_m + [S])$, and [I] is the CPO concentration. The bimolecular rate constant, k_i, was calculated from the ratio k_2/K_d, which is the reciprocal of the slope of the linear curve, $1/k_{obs}$ vs $1/[I]$ $(1 - \alpha)$ (see Eqn 2).

RESULTS AND DISCUSSION

Determination of K_m *for BChE*

Determination of the Michaelis constant (K_m) for BChE is essential for the calculation of the bimolecular rate constant of inhibition by CPO when measured in the presence of substrate. Therefore, the activities of native HS BChE, rH BChE, and its single-site mutant, $A_{328}Y$, were measured at different concentrations of BTC. Figure 1 describes the dependence of enzyme activity on substrate concentration obtained for HS BChE and rH BChE using BTC concentrations between 0.005 and 7 mM. The various parameters (K_m, K_{ss} and b) were calculated by a nonlinear fit according to Eqn 1 (Materials and Methods) and are summarized in Table 1. The K_m values obtained for HS BChE and rH BChE were 10 and 12 μM, respectively. The experimental data obtained for rH BChE were reanalyzed using either Eqn 3 or Eqn 4, which includes the dissociation constant of a substrate–enzyme complex at the peripheral site (K_{ss}) [18]:

$$v = V_{max}/(1 + K_m/S) \quad (3)$$

$$v = V_{max}/(1 + K_m/S + S/K_{ss}) \quad (4)$$

The K_m values calculated according to three different equations, 1, 3, and 4, for rH BChE were 12, 28.5, and 14.5 μM, respectively. The K_m value for rM BChE is 35 μM, using BTC as substrate and Eqn 4 for analysis [14]. The K_m for wild-type rH AChE using ATC is 0.14 mM and the K_m of its double mutant, $F_{295}L/F_{297}V$, using BTC is 0.03 mM [11]. These K_m values and those obtained for HS BChE and rH BChE by nonlinear fit using Eqn 1 (see Fig. 1) were used for the calculation of the bimolecular rate constant of inhibition by CPO in the presence of substrate (see Table 2).

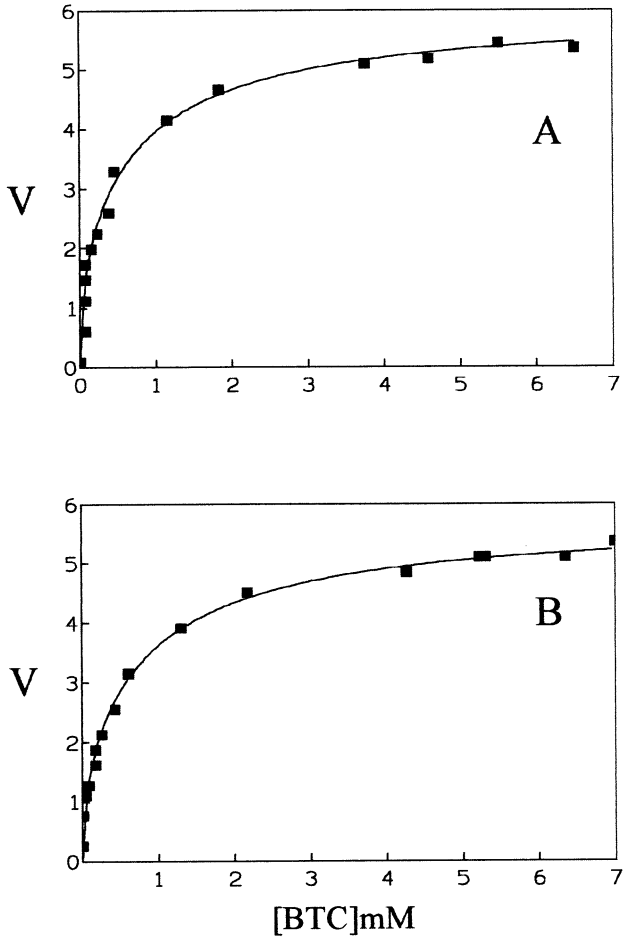

FIG. 1. Concentration dependence for BTC hydrolysis by human BChE. BChE activity was measured according to the procedure of Ellman [13] at specified butyrylthiocholine (BTC) concentrations (0.005 to 7 mM). (A) rH BChE. (B) Purified HS BChE. The slope of absorbance (at 412 nm)/min was taken as the enzyme activity at each BTC concentration. Nonlinear fit to the experimental data was performed using Eqn 1. The values of the kinetic parameters obtained for HS and rH BChE are summarized in Table 1.

Inhibition of AChE by Paraoxon and CPO

Paraoxon was used as a reference inhibitor since it forms the same diethylphosphoryl-AChE conjugate and differs from CPO only by its leaving group (Scheme 1), *p*-nitrophenyl as compared with 2-hydroxy 3,5,6-trichloro pyridyl. The bimolecular rate constants (k_i) for the inhibition of AChE from various species by CPO and paraoxon are summarized in Table 2. The values of k_i for the inhibition of paraoxon of FBS AChE, rM AChE, *Torpedo* AChE (dimeric form) and rH AChE were 3.2, 4.0, 0.6, and 7.0×10^5 M^{-1} min^{-1}, respectively (Table 2). The k_i values obtained for the inhibition by CPO of FBS, rM, human RBC, rH and *Torpedo* AChE (k_i = 2.2–9.37 $\times$ 10^6 M^{-1} min^{-1}, Table 2) were larger than those determined for paraoxon. These values are in good agreement with k_i values obtained for inhibition of brain AChE of various mammalian species [20]. Figure 2 describes the time course of FBS-AChE inhibition by paraoxon and CPO in the absence of substrate, using the sampling method (see Materials and Methods). Prolonged incubation of AChE and BChE from various sources with CPS (0.01 to 0.001 mM) resulted in marginal inhibition (<10%, not shown).

Inhibition of BChE by Paraoxon and CPO

The inhibition of HS BChE by paraoxon and CPO was first measured by using the sampling method. The bimolecular rate constants obtained for the inhibition of rM BChE, HS BChE, and rH BChE by paraoxon were 2.5, 1.9, and 1.6 $\times$

TABLE 1. Kinetic parameters for the hydrolysis of BTC by human BChE

Enzyme	V^*_{max}	b†	K_{ss} (mM)	K_m (mM)
rH BChE (wild-type)	2 ± 0.2	2.8 ± 0.3	0.9 ± 0.1	0.012 ± 0.002
HS BChE	1.8 ± 0.2	3 ± 0.3	1 ± 0.1	0.010 ± 0.002

Parameters were calculated from experimental data (average of three experiments ± SEM) using Eqn 1.
*V_{max} values in OD_{412}/min/mL correspond to 0.470 and 0.423 units/mL, respectively.
†b is the activation factor of BChE for the ternary complex, ESE (see Scheme 2) [15].

10^6 M^{-1} min^{-1} (Table 2). These values are based on initial-rate kinetic measurements where spontaneous reactivation of diethylphosphoryl-BChE is negligible. While inhibition of BChE by paraoxon (in the absence of substrate) could be followed progressively with time (Fig. 3), the inhibition by CPO resulted in an immediate decrease in BChE activity that depended on CPO concentration (not shown). Since the time course of the sampling method was insufficient for monitoring the rapid interaction of CPO with BChE, inhibition by CPO was followed in real-time in the presence of substrate. The k_i values obtained for the inhibition of rM BChE, HS BChE, and rH BChE by CPO were 0.78, 1.65, and 1.67 × 10^9 M^{-1} min^{-1}, respectively (Table 2). The k_i value obtained for inhibition by CPO of the single mutant $A_{328}Y$ of rH BChE, that displays AChE characteristics with respect to inhibition by Huperzine A [21], was 21-fold lower than that obtained for wild-type rH BChE (7.9 × 10^7 vs 1.67 × 10^9 M^{-1} min^{-1}, Table 2). In contrast, the k_i obtained for the inhibition of mutant $A_{328}Y$ BChE by paraoxon was similar to that of rH BChE (1.7 and 1.6 × 10^6 M^{-1} min^{-1}, Table 2). Because the crystal structure of BChE has not been resolved thus far, one may only extrapolate from the three-dimensional structure of *Torpedo* AChE [22]. Substitution of alanine 328 by tyrosine (that parallels to tyrosine 337 in mammalian AChE) may result in steric hindrance toward CPO due to a larger volume of the tyrosine side chain as compared with alanine. The marked difference between the bimolecular rate constants of mammalian AChE and BChE inhibition by CPO, between 160- and 750-fold (Table 2), together with the exceptionally large k_i value for BChE inhibition by CPO, renders CPO a selective inhibitor for quantitative determi-

TABLE 2. Bimolecular rate constants of cholinesterase inhibition by CPO and paraoxon

	k_i × 10^6 (M^{-1} min^{-1})	
Enzyme	CPO	Paraoxon
FBS-AChE	2.2 ± 0.2	0.32 ± 0.10
Human RBC AChE	3.8 ± 0.1	ND
Torpedo AChE (dimer)	8.0 ± 2.0	0.06 ± 0.02
rM AChE (wt)	5.1 ± 1.4	0.4 ± 0.15
rH AChE (wt)	9.3 ± 0.9 (10 ± 1*)	0.7 ± 0.3
$F_{295}L/F_{297}V$ rH AChE	1500 ± 160*	2.0 ± 0.4†
Human serum BChE	1655 ± 25*	1.9 ± 0.03
rH BChE (wt)	1667 ± 59*	1.6 ± 0.4
$A_{328}Y$ rH BChE	78.6 ± 3.8*	1.7 ± 0.2
rM BChE (wt)	780 ± 56*	2.5 ± 0.5

All k_i values (means ± SEM) were determined from at least three different experiments. ND = not determined.
*The k_i value was determined in the presence of substrate.
†Ordentlich *et al.* [19].

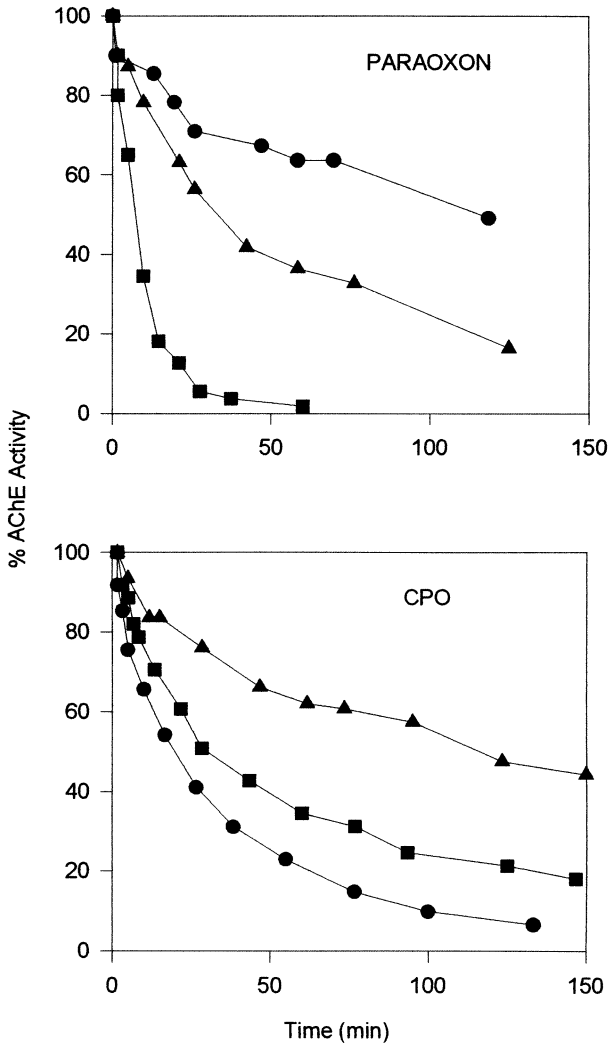

FIG. 2. Time course of FBS-AChE inhibition by paraoxon and CPO. FBS-AChE (5 U/mL; 0.013 nmol) was incubated for specified time intervals with either paraoxon or CPO (50 mM phosphate, pH 8, 0.01% BSA, 25°). Aliquots (20 μL) were assayed for residual AChE activity [13] in 3-mL cuvettes (final AChE concentration was 0.033 U/mL) containing DTNB (1 mM) and ATC (0.5 mM). The inhibition kinetic curves represent data obtained from three experiments. The upper panel describes the time course of FBS-AChE inhibition by paraoxon (●, 50 nM; ▲, 100 nM; and ■, 500 nM). The lower panel describes the time course of inhibition by CPO (▲, 4.5 nM; ■, 9 nM; and ●, 13.5 nM).

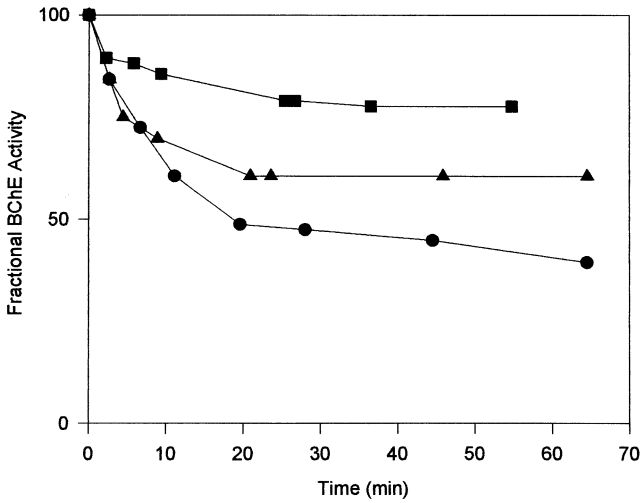

FIG. 3. Time course of HS BChE inhibition by paraoxon. HS BChE (75 μL of 1.3 U/mL; final concentration: 1.6 pmol/mL) was incubated with paraoxon at (■) 18 nM, (▲) 36 nM, and (●) 55 nM for specified time intervals in 1 mL of 50 mM phosphate, 0.01% BSA, pH 8, 25°. Aliquots (50 μL) of the inhibited enzyme solution were assayed for residual BChE activity by Ellman's assay [13] in the presence of 0.5 mM BTC and 1 mM DTNB. At longer time periods (6–24 hr) the enzyme inhibition increased to 70–90%, depending on paraoxon concentration (data not shown).

nation of BChE active-site concentration. It should be noted that the k_i obtained for rH AChE inhibition with CPO by using either the sampling or direct method was 10^7 M^{-1} min^{-1} (Table 2). Iso-OMPA (tetraisopropyl pyrophosphoramide), an organophosphorus inhibitor widely used for selective inhibition of BChE [23], inhibits mouse BChE with a bimolecular rate constant of 2.2×10^5 M^{-1} min^{-1}, compared with a much lower k_i with mouse AChE, 15.6 M^{-1} min^{-1} [15]. However, the k_i obtained for iso-OMPA with mouse BChE was more than three orders of magnitude smaller than the k_i obtained for CPO with rM BChE, 7.8×10^8 M^{-1} min^{-1} (Table 2). Therefore, CPO may serve as a marker of BChE in muscle and nervous tissues of certain species, especially in regions where BChE levels are minute. Due to the rapid reaction between CPO and BChE, it is conceivable that BChE may also serve as an efficient endogenous scavenger of CPO that is released into the blood following metabolic oxidative desulfuration of CPS. In severe poisoning caused by CPS, it may also be advisable to use exogenous BChE as a scavenger that will prevent delayed cholinergic toxic signs caused by newly formed CPO. Because CPO and paraoxon inhibit AChE with similar bimolecular rate constants and the rate of their hydrolysis by A-esterases is similar (not shown), the more rapid reaction of CPO with BChE, resulting in a more rapid scavenging of CPO than of paraoxon, may account for the significantly lower toxicity of the parent phosphorothionate insecticide CPS (LD_{50} = 155 mg/kg, per os in male rats) as compared with parathion (LD_{50} = 13 mg/kg, per os, male rats) [24].

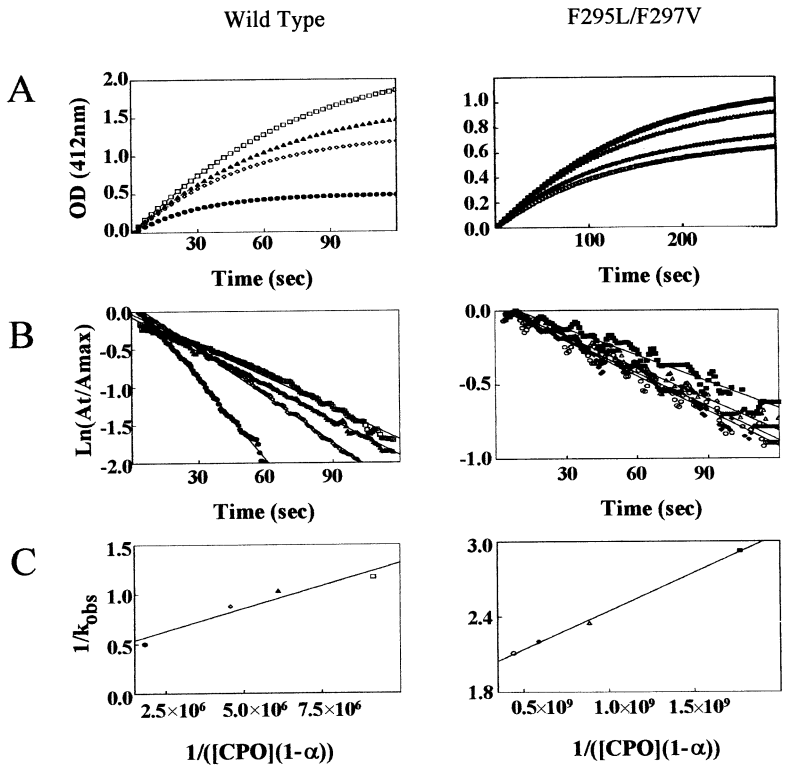

FIG. 4. Progressive inhibition curves and derivation of the kinetic parameters for inhibition of rH AChE wild type and $F_{295}L/F_{297}V$ mutant by CPO in the presence of substrate (wt: 0.5 mM ATC; double mutant: 0.5 mM BTC). The activity of rH AChE samples was measured in 100 μL total reaction volume with 0.5 mM ATC and 1 mM DTNB in 50 mM phosphate, pH 7.5, using a Thermomax microplate reader set at 25°. Determination of the bimolecular rate constants for inhibition by CPO of wild-type human AChE and its double mutant $F_{295}L/F_{297}V$ was performed using the double-reciprocal method of Hart and O'Brien [16], as detailed previously [17], using Eqn 2. (A) Direct reading of wild-type rH AChE activity (OD_{412}) and of its double mutant $F_{295}L/F_{297}V$ at various CPO concentrations (0.25 to 1 μM and 10 to 40 nM, respectively). (B) Linear plots obtained from the log derivatives of the curves in panel A. The derivatives were obtained from the nonlinear functions of the activity curves using the INPLOT4 software program. (C) Double-reciprocal plot of $1/k_{obs}$ vs $1/[CPO](1 - \alpha)$ according to Hart and O'Brien [16]. CPO concentrations used for the inhibition of wild-type rH AChE were (□) 0.5, (▲) 0.75, (◇) 1.0, and (●) 2.5 μM. CPO concentrations used for the inhibition of the double mutant AChE were: (■) 10, (△) 20, (◆) 30, and (○) 40 nM. The K_m values used for the calculation of α were 0.14 mM for rH AChE (ATC) and 0.03 mM for the $F_{295}L/F_{297}V$ double mutant (BTC) [11].

TABLE 3. Kinetic parameters for the inhibition of recombinant human AChE and its acyl pocket mutants by CPO

Enzyme	Substrate (0.5 mM)	CPO (nM)	k_2 (min^{-1})	K_d (nM)	$k_i \times 10^8$ (M^{-1} min^{-1})	k_i/k_i (wt)
Wild type	ATC	250–1000	2.5 ± 0.4	229 ± 46	0.1 ± 0.02	1.0
$F_{295}A$	ATC	5–50	1.4 ± 0.3	1.9 ± 0.4	7.3 ± 1.5	73
$F_{297}A$	ATC	5–50	1.3 ± 0.4	18.3 ± 0.6	0.7 ± 0.2	7
$F_{295}L/F_{297}V$	BTC	10–40	0.6 ± 0.03	0.4 ± 0.05	15.0 ± 1.6	150

Values for k_2, K_d, and k_i are means ± SEM calculated from three repeated experiments.

Inhibition of Human AChE and its Acyl Pocket Mutants by CPO

It was shown previously that double-site mutation of the phenylalanine residues residing at the acyl pocket of AChE active center at position 295 and 297 confers BChE character [11, 15, 25]. Therefore, it was of interest to measure the rate of inhibition by CPO with single- and double-site mutants of these phenylalanine residues. The time course of inhibition by CPO of wild-type rH AChE, single-site mutants $F_{295}A$ and $F_{297}A$ (not shown), and the double mutant $F_{295}L/F_{297}V$ was measured in the presence of substrate (ATC or BTC). The time course of ATC (or BTC) hydrolysis by the wild-type and the double mutant $F_{295}L/F_{297}V$, in the presence of various concentrations of CPO, is shown in Fig. 4A. The pseudo-first-order rate constant, k_{obs}, was calculated from the semi-logarithmic plot of activity versus time presented in Fig. 4B. The double-reciprocal plots of $1/k_{obs}$ vs $1/[I](1 - \alpha)$ for the wild-type and double mutant are described in Fig. 4C. The values of k_i obtained for wild-type rH AChE and its acyl pocket mutants are summarized in Table 3. The K_m values for ATC and BTC hydrolyzed by the various mutants were determined previously [11]. The largest value of the ratio k_i/k_i (wt) = 150 (Table 3) was obtained for the double mutant $F_{295}L/F_{297}V$, which displays characteristics of BChE. The 150-fold difference in k_i values between the double mutant $F_{295}L/F_{297}V$ and the wild type stems primarily from a 572-fold lower K_d for the double mutant (0.4 nM, Table 3) as compared with the wild type (229 nM, Table 3). The difference in K_d reflects higher affinity of CPO for the double mutant acyl pocket, resulting in the formation of a more stable reversible EI complex prior to the covalent phosphorylation step. The relative invariance of k_2 as compared with the difference in K_d was demonstrated recently for other organophosphates [19]. The bimolecular rate constants for inhibition of the single-site mutants $F_{295}A$ and $F_{297}A$ were 73- and 7-fold larger than for the wild type, respectively (Table 3). This difference is in good agreement with the values of the bimolecular rate constants of BTC hydrolysis (k_{cat}/K_m) obtained for the single mutants $F_{295}A$ and $F_{297}A$ (33.3×10^8 vs 1.4×10^8 M^{-1} min^{-1}, respectively) [11], suggesting that residue 295 is the major contributor to the improved interaction of BTC with the mutant enzyme. Accordingly, the $F_{295}A$ mutant was inhibited by CPO at about a 10-fold higher rate than the $F_{297}A$ mutant ($k_i = 7.3 \times 10^8$ and 0.7×10^8 M^{-1} min^{-1}, respectively, Table 3). The difference in the rates of inhibition between AChE and BChE may be explained by better fit of the bulky leaving group of CPO (3,5,6-trichloro-2-pyridyl) to a certain subsite(s) of the catalytic center of BChE than to that of AChE. Indeed, the acyl pocket double mutant of rH AChE displayed better reactivity towards CPO than the wild-type enzyme. This fit may facilitate the formation of a stable reversible enzyme-inhibitor Michaelis complex between CPO and BChE as evidenced by a smaller K_d value obtained for the double mutant. Furthermore, the increased rate of inhibition by CPO obtained for the acyl pocket double mutant provides a rationale for higher efficacy of CPO scavenging by BChE compared with AChE. This does not exclude other residues that could contribute to the differential reactivities of the two enzymes toward CPO, e.g. replacement of Y_{337} in AChE by alanine may also increase the rate of inhibition by CPO as indicated by a decrease in rate obtained from the parallel single site mutant $A_{328}Y$ of rH BChE (Table 2). It remains to be determined how the different leaving groups of CPO and paraoxon have such a remarkable effect on the inhibition rate of the two enzymes.

We wish to thank Drs. A. Shafferman, B. Velan, Z. Radic, P. Taylor, O. Lockridge, and A. Saxena for helpful discussions. Dr. G. Amitai was the recipient of a senior National Research Council fellowship at WRAIR.

References

1. Chambers JE and Chambers HW, Oxidative desulfuration of chlorpyrifos, chlorpyrifos–methyl, and leptophos by rat brain and liver. *J Biochem Toxicol* **4:** 201–203, 1989.
2. Osterloh J, Lotti M and Pond SM, Toxicologic studies in a fatal overdose of 2,4-D, MCPP, and chlorpyrifos. *J Anal Toxicol* **7:** 125–129, 1983.
3. Sultatos LG, Shao M and Murphy SD, The role of hepatic biotransformation in mediating the acute toxicity of the phosphorothionate insecticide chlorpyrifos. *Toxicol Appl Pharmacol* **73:** 60–68, 1984.
4. Costa LG, McDonald BE, Murphy SD, Omenn GS, Richter RJ, Motulsky AG and Furlong CE, Serum paraoxonase and its influence on paraoxon and chlorpyrifos-oxon toxicity in rats. *Toxicol Appl Pharmacol* **103:** 66–76, 1990.
5. Richardson RJ, Moore TB, Kayyali US and Randall JC, Chlorpyrifos: Assessment of potential for delayed neurotoxicity by repeated dosing in adult hens with monitoring of brain acetylcholinesterase, brain and lymphocyte neurotoxic

esterase, and plasma butyrylcholinesterase activities. *Fundam Appl Toxicol* **21:** 89–96, 1993.
6. Richardson RJ, Moore TB, Kayyali US, Fowke JH and Randall JC, Inhibition of hen brain acetylcholinesterase and neurotoxic esterase by chlorpyrifos *in vivo* and kinetics of inhibition by chlorpyrifos oxon *in vitro*: Application to assessment of neuropathic risk. *Fundam Appl Toxicol* **20:** 273–279, 1993.
7. Ogawa Y, Suzuki S, Uchida O, Kamata E, Saito M, Umemura T, Wakana M, Kaneko T, Kurokawa Y and Tobe M, 28-Day repeated dose toxicity test of chlorpyrifos in Wistar rat. *Eisei Shikenjo Hokoku* **106:** 48–54, 1988.
8. Corley RA, Calhoun LL, Dittenber DA, Lomax LG and Landry TD, Chlorpyrifos: A 13-week nose-only vapor inhalation study in Fischer 344 rats. *Fundam Appl Toxicol* **13:** 616–618, 1989.
9. Richardson RJ, Assessment of the neurotoxic potential of chlorpyrifos relative to other organophosphorus compounds: A critical review of the literature. *J Toxicol Environ Health* **44:** 135–165, 1995.
10. Kaplan JG, Kessler J, Rosenberg N, Pack D and Schaumberg HH, Sensory neuropathy associated with Dursban (chlorpyrifos) exposure. *Neurology* **43:** 2193–2196, 1993.
11. Ordentlich A, Barak D, Kronman C, Flashner Y, Leitner M, Segall Y, Ariel N, Cohen S, Velan B and Shafferman A, Dissection of the human acetylcholinesterase active center determinants of substrate specificity. Identification of residues constituting the anionic site, the hydrophobic site, and the acyl pocket. *J Biol Chem* **268:** 17083–17095, 1993.
12. De La Hoz D, Doctor BP, Ralston JS, Rush RS and Wolfe AD, A simplified procedure for the purification of large quantities of fetal bovine serum acetylcholinesterase. *Life Sci* **21:** 195–199, 1986.
13. Ellman GC, Courtney KD, Anders V and Featherstone RM, A new and rapid colorimetric determination of acetylcholinesterase activity. *Biochem Pharmacol* **7:** 88–95, 1961.
14. Hosea NA, Berman HA and Taylor P, Specificity and orientation of trigonal carboxyl esters and tetrahedral alkylphosphonyl esters in cholinesterases. *Biochemistry* **34:** 11528–11536, 1995.
15. Vellom D, Radic Z, Li Y, Pickering NA, Camp S and Taylor P, Amino acid residues controlling acetylcholinesterase and butyrylcholinesterase specificity. *Biochemistry* **32:** 12–17, 1993.
16. Hart GJ and O'Brien RD, Recording spectrophotometric method for determination of dissociation and phosphorylation constants for the inhibition of acetylcholinesterase by organophosphates in the presence of substrate. *Biochemistry* **12:** 2940–2945, 1973.
17. Barak D, Ordentlich A, Bromberg A, Kronman C, Marcus D, Lazar A, Ariel N, Velan B and Shafferman A, Allosteric modulation of acetylcholinesterase activity by peripheral ligands involves a conformational transition of the anionic subsite. *Biochemistry* **34:** 15444–15452, 1995.
18. Radic Z, Pickering NA, Vellom DC, Camp S and Taylor P, Three distinct domains in the cholinesterase molecule confer selectivity for acetyl- and butyrylcholinesterase inhibitors. *Biochemistry* **32:** 12074–12084, 1993.
19. Ordentlich A, Barak D, Kronman C, Ariel N, Segall Y, Velan B and Shafferman A, The architecture of human acetylcholinesterase active center probed by interactions with selected organophosphate inhibitors. *J Biol Chem* **271:** 11953–11962, 1996.
20. Wang C and Murphy SD, Kinetic analysis of species difference in acetylcholinesterase sensitivity to organophosphate insecticides. *Toxicol Appl Pharmacol* **66:** 409–419, 1982.
21. Saxena A, Redman AMG, Jiang X, Lockridge O and Doctor BP, Differences in active site gorge dimensions of cholinesterases revealed by binding of inhibitors to human butyrylcholinesterase. *Biochemistry* **36:** 14642–14651, 1997.
22. Sussman JL, Harel M, Frolow F, Oefner C, Goldman A, Toker L and Silman I, Atomic structure of acetylcholinesterase from *Torpedo californica*: A prototypic acetylcholine-binding protein. *Science* **253:** 872–879, 1991.
23. Silver A, *The Biology of the Cholinesterases*. North Holland, Amsterdam, 1974.
24. Gaines TB, Acute toxicity of pesticides. *Toxicol Appl Pharmacol* **14:** 515–534, 1969.
25. Harel M, Sussman JL, Krejci E, Bon S, Chanal P, Massoulié J and Silman I, Conversion of acetylcholinesterase to butyrylcholinesterase: Modeling and mutagenesis. *Proc Natl Acad Sci* **89:** 10827–10831, 1992.